NANO LETTERS

2006
Vol. 6, No. 12
2814−2820

# Single-Pair FRET Characterization of DNA Tweezers

**Barbara K. Müller,[†] Andreas Reuter,[‡] Friedrich C. Simmel,*[,‡] and Don C. Lamb*[,†,§]**

*Physical Chemistry, Department of Chemistry and Biochemistry, and Center for Nanoscience, Ludwig-Maximilians-Universität München, Butenandtstr. 11, Haus E, D-81377 Munich, Germany, Department of Physics and Center for Nanoscience, Ludwig-Maximilians-Universität München, Geschwister-Scholl-Platz 1, D-80539 Munich, Germany, and Department of Physics, University of Illinois at Urbana-Champaign, 1110 West Green Street, Urbana, Illinois 61801*

*Received August 18, 2006; Revised Manuscript Received September 30, 2006*

**ABSTRACT**

**The self-assembly properties of DNA make it an ideal choice for the construction of nanomachines such as DNA tweezers. Because nanomachines function as individual units, they need to be studied on the single-molecule level. From single-pair FRET investigations, we show that "open" tweezers exist in a single conformation with minimal FRET efficiency, whereas upon addition of a "closing strand", three conformations are observed, which are averaged out in ensemble measurements.**

**Introduction.** In recent years, the remarkable self-assembly properties of DNA have been utilized for the fabrication of supramolecular ordered structures[1] and nanomechanical molecular devices.[2] With these devices, it has been demonstrated that DNA can be used to produce simple movements on the nanometer scale such as rotation,[3,4] stretching,[2,5,6] and translocation.[7−11] On the basis of these prototypical devices, more advanced molecular machines are expected to be constructed from DNA, with many possible applications in nanotechnology and biomedicine. DNA nanomachines can be used for the precise and programmable adjustment of distances between molecules[12] or other nanoscale objects,[13] and even for the control of chemical reactions between them.[14,15] These capabilities are extremely important for the realization of nanoscale assembly lines. In biomedicine, DNA nanomachines may find application as advanced biosensors[16−18] and also as DNA-addressable drug-release units.[19−22] It is crucial to perform more thorough structural and dynamical studies on them in order to better understand how these devices function and to improve their design, analogous to those on naturally occurring biological nanomachines. So far, with only a few exceptions (e.g., a study on a "nanometronome"[23]), essentially all FRET investigations of DNA devices were performed on ensembles.

In this communication, we investigate one of the prototype DNA "machines", DNA tweezers,[5] on the single-molecule level by single-pair Förster resonance energy transfer (sp-FRET) measurements. DNA tweezers are composed of three oligonucleotides (Figure 1): a central DNA strand, C, and two other strands, A1 and A2, which hybridize to C to form the two "arms" of the tweezers. The structure is composed of two 18-base-pair- (bp) long double-stranded arms with 24 nucleotide (nt) overhangs for addressing the two arms and a flexible, 4-nt-long "hinge" between the two arms. As indicated in Figure 1, the open tweezer structure can be "closed" by the addition of a DNA "fuel" strand, F, which hybridizes to the overhang on both arms, pulling the arms close together. The fuel strand may be displaced from the tweezers by the addition of a DNA "removal" strand via branch migration. Alternate addition of fuel and removal strands facilitates a cyclical operation of the device.

In previous investigations, DNA tweezers[5] were constructed with a fluorescently double-labeled C strand and investigated using both gel electrophoresis and ensemble FRET measurements. Because of the high sensitivity of Förster resonance energy transfer (FRET) to motions on the nanometer scale, FRET experiments in addition to gel electrophoresis are becoming the standard characterization method of DNA nanomachines. When the tweezers are open, the donor and acceptor are far away and the FRET signal is small. Closing of the tweezers brings the two dyes into close proximity and thus increases energy transfer between the donor and acceptor. These previous experiments showed that DNA tweezers can be switched between their open and

* Corresponding authors. F.C.S.: E-mail: simmel@lmu.de; fax: (+49) 89 2180 3182. D.C.L.: E-mail: don.lamb@cup.uni-muenchen.de; fax: (+49) 89 2180 77560.

[†] Physical Chemistry, Department of Chemistry and Biochemistry, and Center for Nanoscience, Ludwig-Maximilians-Universität München.

[‡] Department of Physics and Center for Nanoscience, Ludwig-Maximilians-Universität München.

[§] University of Illinois at Urbana-Champaign.

10.1021/nl0619406 CCC: $33.50 
**Published on Web 10/27/2006**

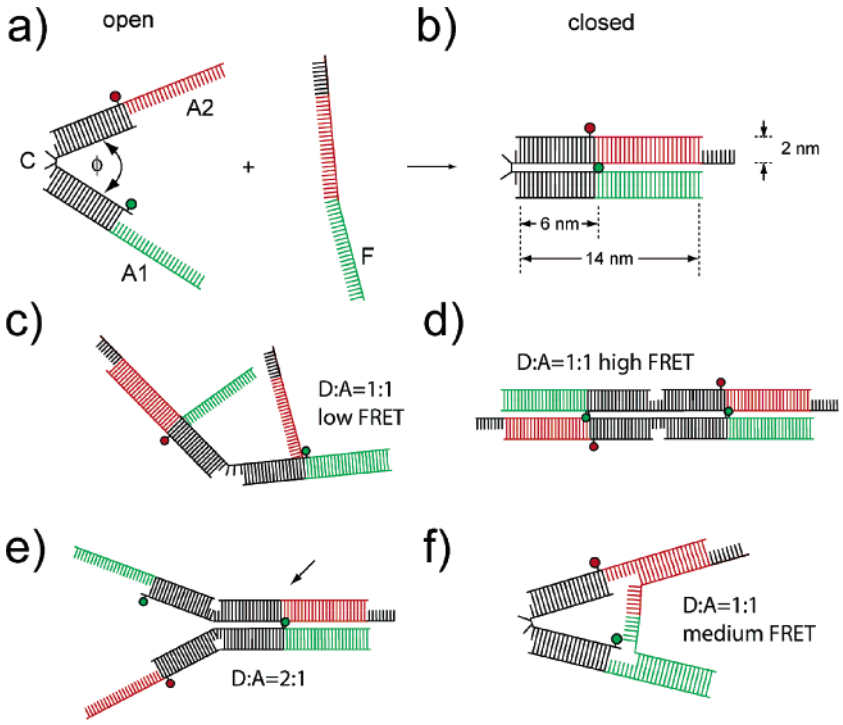


**Figure 1.** Schematic depiction of the DNA tweezers. (a) The open tweezers are formed by three strands of DNA: A1, A2, and C. (b) Upon the addition of a "fuel" strand, F, the two arms are pulled together. (c−f) Unwanted hybridization products resulting from the reaction of fuel strands with the tweezers. (c) Reaction of two fuel strands with one tweezer. (d) Dimer of two tweezers linked by two fuel strands leading to the same relative arrangement of donors and acceptors as expected from ordinarily closed tweezers. (e) Two tweezers linked by one fuel strand. In addition, it is assumed here that one of the tweezers is incompletely labeled. The arrow points to the position of the missing acceptor molecule. (f) A sterically hindered tweezer structure that is only partially closed. Further hybridization of the remaining unpaired nucleotides is prohibited by the double-helical nature of DNA.

closed states many times. In the open state, the mean distance between the ends of the arms was estimated to be around 6 nm, whereas, in the closed state, they are assumed to be almost in contact. Because the fluorescence signal obtained in bulk measurements is an average over many possible arrangements of the fluorescent dye molecules, several issues could not be resolved: (1) How uniform and mechanically robust are the tweezers in the "open" state? (2) How pure is the closed state? (3) How is the FRET signal affected by multimer formation upon addition of the fuel strand (Figure 1c−e)?

To investigate these issues in greater detail, we have performed single-pair FRET measurements on DNA tweezers using pulsed interleaved excitation (PIE),[24] a variation of alternating laser excitation (ALEX).[25] The DNA tweezers were labeled with a donor molecule attached to the 5′ end of the C strand, and the A2 strand was labeled internally on a thymine with the acceptor molecule. PIE enables us to identify those DNA devices that carry two fluorescent labels from those that have only a donor or an acceptor. Using this technique, artifacts originating from singly labeled species can be removed from the data even at low FRET efficiencies and more accurate quantitative conclusions can be drawn. From the spFRET/PIE experiments, we derived information about the distribution of conformations of the tweezers in the different states and investigated the existence of subpopulations in the sample.

**FRET and PIE.** FRET is the radiationless transfer of energy between two dipoles and depends on the spectral overlap of the fluorescence emission spectrum from the donor and absorption spectrum of the acceptor, the relative orientation of the two fluorophores, and their separation.[26] An overview of FRET can be found in the book by Lakowicz.[27] The FRET efficiency is related to the distance, $r$, between the fluorophores as shown in eq 1

$$f_E = \frac{1}{1 + (r/R_0)^6} \quad (1)$$

where $R_0$, the Förster radius, is the distance at which 50% of the energy is transferred to the acceptor. For the fluorophores used in this work, Atto 532 and Atto 647-N, we determined the Förster radius to be $R_0 \approx 5.1$ nm assuming a random orientation between the donor and acceptor dipoles.

Single-molecule fluorescence measurements are typically performed on either a surface using confocal microscopy or wide field techniques or in solution using confocal microscopy. For the measurements reported here, the DNA tweezers were measured in solution at a concentration of ∼20 pM. At this concentration, the probability of a molecule being in the probe volume is approximately 1%, and the probability of two or more molecules being in the probe volume is negligible. A burst analysis[28−30] was performed from the burst of photons detected as molecules traverse the confocal probe volume. The donor and acceptor fluorescence intensities during a fluorescence burst were determined for the individual molecules. The FRET efficiency, $f_E$, was calculated

from the fluorescent intensities of the donor and acceptor molecules using eq 2

$$f_E = \frac{F_{AD}}{\alpha F_{DA} + F_{AD}} \tag{2}$$

where $F_{AD}$ is the fluorescence of the acceptor in the presence of the donor corrected for direct excitation of the acceptor and crosstalk from the donor, $F_{DA}$ is the fluorescence intensity of the donor in the presence of the acceptor dye, and $\alpha = \eta_A\phi_A/\eta_D\phi_D$ is a detection correction factor accounting for the different sensitivities in the donor and acceptor channels. For the results presented here, $\alpha = 1.0$. The separation between donor and acceptor molecules can be calculated directly from the fluorescence intensities using eq 3

$$r = R_0\left(\frac{\alpha F_{DA}}{F_{AD}}\right)^{1/6} \tag{3}$$

To distinguish between double-labeled DNA tweezers with low FRET efficiencies and singly labeled tweezers without a fluorescently active acceptor, we used PIE. The details of the method are given in Müller et al.[24] In PIE, multiple laser sources are alternated with repetition rates in the range of MHz. Here, a green laser and a red laser were alternated with a repetition rate of 10 MHz. With PIE, two measurements are performed virtually simultaneously, one with green excitation and a second with red excitation. When a molecule is present in the probe volume, the measurement with green excitation provides the single-pair FRET information while the measurements with red excitation verify that a fluorescently active acceptor is in the probe volume. Provided that the concentration of tweezers is low enough that no more than one tweezer is in the probe volume at a time, simultaneous bursts with both green and red excitation verify that the molecule traversing the probe volume has both an active donor and an acceptor molecule.

**Results.** The correct formation and closure of the tweezers structure is strongly dependent on the reaction conditions as seen with nondenaturing 9% polyacrylamide gel electrophoresis (PAGE, Figure 2). Lane a contains the open tweezer structure composed of strands C, A1, and A2, after a high-temperature annealing step (5 min at 90 °C followed by cooling to 4 °C over ~1.5 hrs) in TE buffer. The predominant band is the open tweezers, but there are also incomplete structures composed of C and only one of strands A1 or A2. Lanes b and c contain the results of the hybridization reaction of the sample from lane a with fuel strand F for 1 h in TE buffer, and in TE buffer with 1 M NaCl, respectively. The reaction under low salt conditions has not yet been completed after 1 h, and there is still a considerable amount of fuel strand, F, left unhybridized. In both cases, a strong, high-molecular-weight (MW) band is visible corresponding to the closed tweezers structure. Several other high MW bands occur, which are attributed to multimer structures as exemplified in Figure 1c−e. Lane d contains open tweezers formed

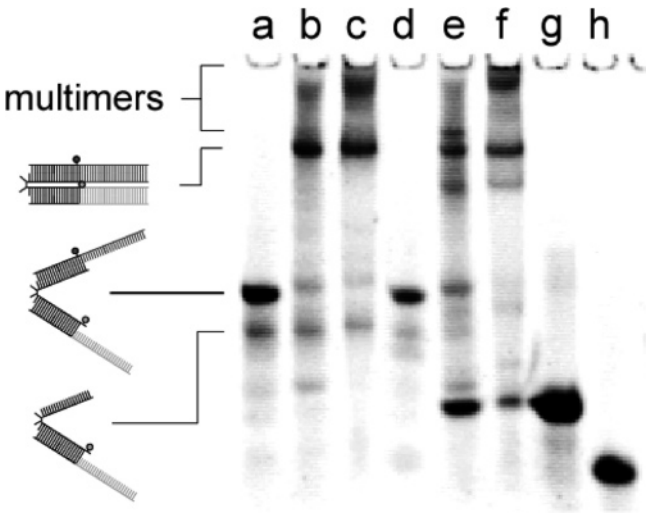


**Figure 2.** Polyacrylamide gel electrophoresis of open and closed tweezers prepared under a variety of conditions. (a) A tweezer sample prepared by high-temperature annealing (see the text) of strands C, A1, and A2 in TE buffer. (b) Result of the addition of a stoichiometric amount of fuel strand F for 1 h at room temperature to the sample in lane a in TE buffer. (c) Same as b, but in TE buffer + 1 M NaCl. (d) A tweezer sample prepared in TE buffer at room temperature without annealing by first hybridizing the C and A1 strands for 1 h, followed by 1 h hybridization of the C-A1 complex with the A2 strand. (e) An equimolar amount of fuel strand F was added to the sample from lane d at room temperature and incubated for 1 h in TE buffer. (f) Same as lane e, but with 1 M NaCl salt in the buffer. (g) Fuel strand F. (h) Strand A1.

in TE buffer without a high-temperature annealing step by mixing equal amounts of strands C and A1 together for 1 h and then adding an equimolar amount of strand A2 to the mixture and incubating for an additional hour. The fuel strand, F, was added to the sample from lane d and incubated for 1 h at room temperature in TE buffer (lane e) and in TE buffer containing 1 M NaCl (lane f). The results of these closing reactions lead to very different distributions among the different species in the reaction volume. Figure 2 shows that the composition of a DNA tweezer's sample contains a complex distribution of a variety of different structures formed by the component strands of the tweezer and depends on the history of the sample, the buffer conditions, annealing procedure, and reaction time. In a bulk fluorescence experiment, a superposition of the various fluorescence signals exhibited by these species will be measured, making it difficult to obtain quantitative statements about the properties of a single species. To resolve this problem, we investigated DNA tweezers on the single-molecule level.

Single-pair FRET measurements were performed in order to obtain a better quantitative understanding of the tweezers' conformation in the "floppy" open state and to gain further insight into the distribution of subpopulations in the sample of closed tweezers. Histograms of the FRET efficiency and donor−acceptor separation obtained from open DNA tweezers at four different salt concentrations (no added salt, 10 mM NaCl, 100 mM NaCl, and 1 M NaCl) are shown in Figure 3. The open tweezers correspond to the sample in

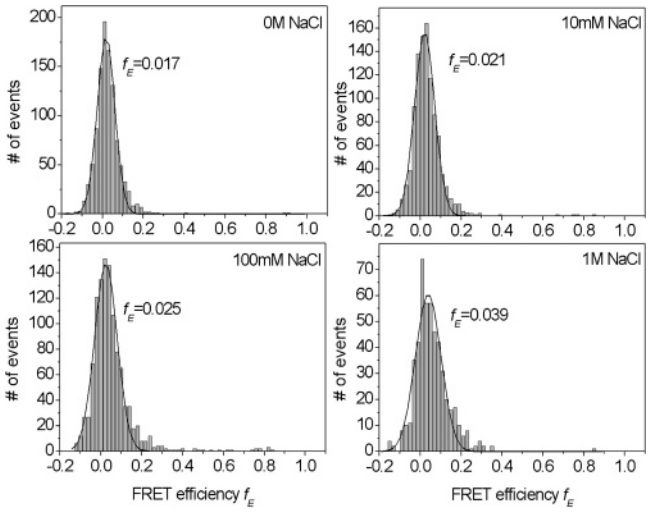


**Figure 3.** FRET efficiency histograms obtained from a burst analysis of spFRET/PIE experiments on open tweezers in buffer with 0 mM, 10 mM, 100 mM, and 1 M NaCl. At higher salt concentrations, the maximum FRET efficiencies shift to higher values, i.e., the average dye-to-dye distances decrease from at least 10.0 nm to roughly 8.7 nm (see the text). The distributions of the efficiencies/distances are unimodal. A Gaussian fit has been made to the data in each case (solid lines).

lane a of Figure 2 with a subsequent 50 000-fold dilution in the corresponding buffer. In each case, a unimodal distribution is obtained. As expected from previous bulk experiments, the FRET efficiencies are low in the open state of the tweezers. Gaussian fits to the FRET efficiency histograms in Figure 3 peak at 1.7%, 2.1%, 2.5%, and 3.9% for 0 mM, 10 mM, 100 mM, and 1 M NaCl, respectively. Experiments performed at different salt concentrations on the same fluorophores attached via a polyproline linker showed no changes in FRET efficiency, verifying that the properties of the fluorophores and buffer do not change significantly with salt. The donor−acceptor separation calculated from the peak of the FRET efficiency yields 10.0, 9.7, 9.4, and 8.7 nm for 0 mM, 10 mM, 100 mM, and 1 M NaCl concentrations, respectively. High-precision distance measurements with FRET require an accurate determination of $R_0$. We determined $R_0$ for the fluorophores we used attached to the DNA tweezers under experimental conditions ($R_0 = 5.1$ nm) and assumed an orientational factor of $^2/_3$. These distances are compatible with earlier results obtained in bulk experiments.[5] Although we have determined the distances to the highest accuracy possible, the absolute values can only give a rough idea of the actual D−A separation and none of the results presented here depend upon the absolute value of the donor−acceptor separation. PIE ensures that the low FRET efficiency we measure is only coming from DNA complexes that contain fluorescently active donor and acceptor molecules. To determine the minimum resolution of our spFRET/PIE system, we performed a test experiment with 60 bp dsDNA labeled at its 5′ and 3′ ends with a similar dye pair (Atto 532, Atto 647). The FRET efficiency obtained for this structure with a nominal dye-to-dye distance of ∼20 nm was $f_E = 2.2\%$, signifying the detection limit of our FRET measurements. This indicates that the distance between the dye labels of the tweezers at 0 M NaCl may also be larger than 10.0 nm. However, a decrease in the distance between the arms after the addition of NaCl to the buffer was observed consistently in all of the experiments performed. This trend is explained easily by the mutual electrostatic repulsion of the two highly charged arms of the tweezers. The relevant length scale over which the arms electrostatically repel each other, the Debye screening length

$$l_D = \sqrt{\frac{\epsilon_r \epsilon_0 k_B T}{2 \times 10^3 e^2 N_A c}}, \quad (4)$$

where $c$ is the concentration of monovalent ions in mol/L, drops from almost 10 nm at 1 mM salt to just 0.3 nm at 1 M salt concentration. The idea that static repulsion between the DNA arms influences the conformational dynamics of the DNA tweezers is consistent with the fact that in measurements without added salt fluorescence signals corresponding to energy transfer efficiencies higher than ∼30% were only rarely observed. At higher salt concentrations, particularly 100 mM, the arms of the tweezers occasionally seem to come close to each other as indicated by a finite number of counts at events with higher FRET efficiencies.

A very different distribution of FRET efficiencies is obtained for the "closed" tweezers. SpFRET/PIE measurements were performed on the same sample of tweezers used for lane c in Figure 2, and the resulting FRET histogram is shown in Figure 4a. Three subpopulations are observed: A high efficiency peak ($f_E = 90.0\%$) due to the reduced distance between the fluorophores in the closed state, a low FRET species ($f_E = 4.2\%$), and, remarkably, a considerable number of molecules with a broadly distributed intermediate value for the FRET efficiency ($f_E = 37.7\%$). The corresponding distance distribution is shown in Figure 4b.

The high-FRET fraction corresponds to a dye-to-dye distance of ∼3.5 nm. This value is consistent with earlier findings and is dependent on the actual relative position of the dyes in the closed state. A priori, for closed tweezers this distance is expected to be anywhere in the range between 0 and 6 nm (i.e., between 0−2 diameters of the DNA duplex plus/minus dye spacer lengths). The same FRET efficiency, however, is also expected for dimers of tweezers composed of two tweezer structures held together by two fuel strands (cf. Figure 1d).

The low FRET efficiency fraction displays the same $f_E$ value as the open tweezers. However, the low-FRET peak does not disappear even when the closing strand, F, is added in excess over the tweezers, suggesting that this fraction cannot be explained by a subpopulation of "still open" tweezers. As we are using PIE, the analyzed complexes have active donor and acceptor molecules, ruling out the possibility of the low FRET peak arising from a donor-only species. One possible explanation is that a fraction of open tweezers binds to two fuel strands (Figure 1c). The probability of binding two fuel strands may be higher than expected due to the fact that the arms of the open strands rarely fluctuate close to each other, as seen from the single-

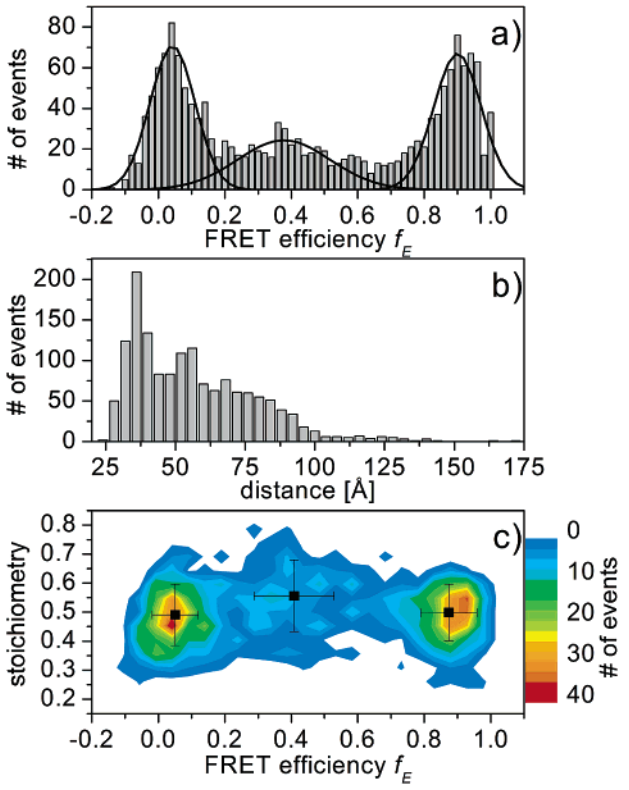


**Figure 4.** (a) FRET efficiency and (b) distance histogram for closed tweezers in TE buffer at 1 M NaCl. Three subpopulations are observed: a pronounced high FRET efficiency ($f_E$) peak, a broad distribution of intermediate $f_E$ values, and a low FRET efficiency peak. These fractions contain contributions from a variety of constructs in the "closed" tweezer sample (cf. text). The high-FRET peak contains properly closed tweezer structures and perhaps dimers in which the donor and acceptor dyes are spatially separated by about 3.5 nm (Figure 1d). The low and intermediate efficiency fractions also contain multimers, but with different ratios of tweezers and fuel strands, and/or incomplete donor and acceptor labeling. In addition, incompletely closed tweezers may also be observed. (c) An analysis of the stoichiometry of dye labeling, eq 5, corresponding to the FRET efficiencies in Figure 4a. The intermediate efficiency fraction has a slightly elevated stoichiometry value, indicating contributions from dimer structures that contain more donor dyes than acceptor molecules. The three black squares with error bars represent the mean value and standard deviation of the FRET efficiency and stoichiometry for molecules with a FRET efficiency below 0.2, between 0.2 and 0.7, and above 0.7.

pair FRET distributions. Another possible explanation for the low FRET fraction of the "closed" tweezers is incomplete dimer formation, for example, when one fuel strand links together two tweezer structures (Figure 1e).

SpFRET/PIE measurements reveal the existence of the third, medium FRET efficiency subpopulation. The spFRET/PIE scheme also allows us to calculate the labeling stoichiometry as defined in Lee et al.[31] (number of donor molecules/total number of dyes) for the various FRET efficiency values (Figure 4c). The stoichiometry factor is given by

$$S = \frac{\alpha F_{DA} + F_{AD}}{\alpha F_{DA} + F_{AD} + F_{AA}} \qquad (5)$$

where $F_{AA}$ is the fluorescence intensity of the acceptor with direct (635 nm) excitation. Although the low and high FRET efficiency fractions are approximately equally labeled with donor and acceptor dyes, the medium FRET fraction shows a shift toward higher stoichiometry values, that is, the structures contain more donors than acceptors. Because the average stoichiometry value of the intermediate FRET population is between ~0.5 and ~0.7, the stoichiometry of this state is mixed. This suggests that the medium FRET fraction arises, in part, from dimers such as the one depicted in Figure 1e, in which one acceptor dye is missing or nonfluorescent. Another component of this subpopulation has 1:1 stoichiometry and may be due to incomplete closure of the tweezers by the fuel strand, as indicated in Figure 1f. When a fuel strand simultaneously hybridizes to both of a tweezer's arms, the topology may be such that complete hybridization is sterically hindered due to the helical nature of duplex DNA. The low and medium FRET efficiency values may also be due to dimerization of incompletely labeled tweezers, a situation that cannot be ruled out even with PIE.

It is possible to extract information about the stability of the DNA tweezers in both the open and closed states by using single-molecule spectroscopy. The labeling scheme we used here is ideal for visualizing the function of the tweezers. The FRET efficiency is very high in the closed state (90%) and goes to virtually zero in the open state. For investigating the dynamics of the tweezers within the open and closed states, the FRET signal in these conformations should be roughly 50%. Hence, new DNA constructs with fluorescent dyes in different positions that are more sensitive to changes in the FRET signal are necessary to investigate the dynamics of the tweezers in different states. From the single-molecule measurements with PIE, we were able to resolve different subpopulations. Although different oligomers are also observed in the PAGE gel, with the single-molecule measurements we were able to determine the FRET efficiency of the different subpopulations, gaining additional information about the structures of these subpopulations. In addition, the FRET efficiencies that we determine for the closed and open tweezers are not affected by incomplete labeling or this intermediate subpopulation. In contrast to values obtained from bulk experiments, the spFRET/PIE efficiencies can be used for accurate distance determinations.

In conclusion, we have performed single-pair FRET studies on a prototype DNA nanomechanical device, DNA tweezers, using the recently introduced experimental scheme of pulsed interleaved excitation. In contrast to earlier bulk experiments, it was possible to deduce the distribution of the tweezers' conformations in the open state, to study the influence of monovalent cations on these distributions, and to identify subpopulations in a sample of closed tweezers. In the open state, the distance between the dye labels on the arms of the tweezers is distributed around 8−10 nm with a fwhm of ~2.5 nm. In the closed state, three subpopulations are observed. The high FRET subpopulation has an average donor−acceptor separation of 3.5 nm, corresponding to properly closed tweezers or dimers of tweezers. In addition to a high FRET efficiency fraction, there is a considerable

fraction of structures displaying low and medium FRET efficiencies. These subpopulations may be due to incompletely closed tweezers, incompletely labeled structures, and tweezers linked together in multimers. This study exemplifies how single-molecule experiments provide additional insight into the structural diversity of an apparently simple nanodevice, DNA tweezers. This information is essential to improve critical points such as stability, integrity, fluctuations, and the uniqueness of these structures. For example, the optimal conditions (DNA and salt concentrations) for preparing the tweezers and the sequence and length of the DNA used to close the tweezers can be systematically studied to minimize aggregation and misfolding in the closed state. We have demonstrated the potential of single-molecule techniques for investigating nanomachines and believe that the incorporation of single-molecule methods will have an enormous impact on the development of nanodevices.

**Experimental Section.** *DNA Sequences.* Oligonucleotides were synthesized and labeled by IBA Technologies, Göttingen, Germany. The sequences are C: 5′-**Atto 532**-TGCCTTGTAAGAGCGACCATCAACCTGGAATGCTTC-GGAT-3′; A1: 5′-GGTCGCTCTTACAAGGCACTGGTAA-CAATCACGGTCTATGCG-3′; A2: 5′-GGAGTCCTACTGTCT-GAACTAACGA**t**CCGAAGCATTCCAGGT-3′, labeled with Atto 647-N at the thymidine at position 26, shown in bold type; and F: 5′-CGCATAGACCGTGATTGTTACCAGCGT-TAGTTCAGACAGTAGGACTCCTGCTACGA-3′. Atto dyes are from Atto-Tec GmbH (Siegen, Germany); all other chemicals are from Sigma-Aldrich (Taufkirchen, Germany).

*Preparation of DNA Tweezers.* DNA tweezers were prepared at a concentration of 1 $\mu$M in TE (Tris-EDTA, pH 8.0) buffer from equimolar solution of strands C, A1, and A2. The closed tweezers were prepared by subsequently adding strand F in a stoichiometric amount. For spFRET measurements, the samples were diluted in the appropriate buffers (TE + NaCl) to a final concentration of approximately 20 pM.

*Gel Electrophoresis.* Nondenaturing gel electrophoresis was performed in a 9% polyacrylamide gel using a TBE (Tris-borate-EDTA, pH 8.5) running buffer at 15−40 V/cm for 2 h.

*SpFRET/PIE Experiments.* SpFRET experiments were performed as described in ref 24. Briefly, the sample is illuminated using two laser light sources, a continuous-wave Argon Krypton Ion Laser (531 nm, Stabilate 2018, Spectra Physics, Darmstadt, Germany) that is pulsed by an acousto-optic modulator (N23080-2-LTD, NEOS Technologies, Melbourne), and a pulsed laser diode (635 nm, Sepia LDH635, PicoQuant, Berlin, Germany). The laser intensities at the sample were 80 $\mu$W for both 531 and 635 nm excitation. The excitation pulses were synchronized to a master clock with a frequency of 10 MHz, and one pulse is delayed with respect to the other. In this way, the sample is excited alternately by green and red laser pulses. The photons are detected with two avalanche photodiodes (EG&G Optoelectronics, Vaudreuil, Canada) using a time-correlated single-photon counting card (TimeHarp 200, PicoQuant), which was also synchronized to the 10 MHz master frequency. From the arrival time of the photon with respect to the master clock, it is possible to deduce which excitation source is responsible for generating the detected photon.

The DNA tweezers used in the present experiment were labeled with Atto 532 (donor) and Atto 647-N (acceptor) fluorophores, which are spectrally well separated (3.7% crosstalk from the green channel into the red channel). An excitation pulse at 635 nm selectively excites the Atto 647-N fluorophores and leads to the emission of red fluorescence photons. An excitation pulse at 531 nm excites the green fluorophore, leading to emission from either the donor fluorophore, or, via FRET, from the acceptor fluorophore. During the experiment, a single DNA tweezer traverses the probe volume giving rise to a burst of photons. Using PIE, it is possible to separate the photons in the burst coming from green excitation from those generated using red excitation. The burst of photons detected in the green and/or red detection channels upon green excitation occurs when a DNA tweezer with a donor molecule is in the probe volume. A simultaneous burst of photons detected in the red channel with red excitation verifies that a fluorescently active acceptor is in the probe volume. Hence, it is possible to distinguish double-labeled DNA tweezers from singly labeled tweezers, even when there is little or no FRET occurring. Hence, "false counts" originating from incompletely labeled molecules are effectively sorted out in a PIE-based spFRET experiment. In the analysis, a threshold was used to select the bursts for analysis. Using time bins of 2 ms, a minimum of 17 detected photons in the sum of the green and red detection channels after green excitation and 12 photons detected in the red detection channel after red excitation were required.

**Acknowledgment.** We gratefully acknowledge the support of Prof. Christoph Bräuchle. This work has been funded by the Deutsche Forschungsgemeinschaft (Emmy Noether grant DFG SI 761/2-2/3, SFB 486, and SFB 646) and the Center for Nanoscience at the LMU Munich.

## References

(1) Seeman, N. C. *Nature* **2003**, *421*, 427−431.
(2) Simmel, F. C.; Dittmer, W. U. *Small* **2005**, *1*, 284−299.
(3) Mao, C. D.; Sun, W. Q.; Shen, Z. Y.; Seeman, N. C. *Nature* **1999**, *397*, 144−146.
(4) Yan, H.; Zhang, X. P.; Shen, Z. Y.; Seeman, N. C. *Nature* **2002**, *415*, 62−65.
(5) Yurke, B.; Turberfield, A. J.; Mills, A. P.; Simmel, F. C.; Neumann, J. L. *Nature* **2000**, *406*, 605−608.
(6) Chen, Y.; Wang, M. S.; Mao, C. D. *Angew. Chem., Int. Ed.* **2004**, *43*, 3554−3557.
(7) Yin, P.; Yan, H.; G., D. X.; Turberfield, A. J.; Reif, J. H. *Angew. Chem., Int. Ed.* **2004**, *43*, 4906−4911.
(8) Shin, J. S.; Pierce, N. A. *J. Am. Chem. Soc.* **2004**, *126*, 10834−10835.
(9) Tian, Y.; Mao, C. D. *J. Am. Chem. Soc.* **2004**, *126*, 11410−11411.
(10) Tian, Y.; He, Y.; Chen, Y.; Yin, P.; Mao, C. D. *Angew. Chem., Int. Ed.* **2005**, *44*, 4355−4358.
(11) Bath, J.; Green, S. J.; Turberfield, A. J. *Angew. Chem., Int. Ed.* **2005**, *44*, 4358−4361.
(12) Kukolka, F.; Müller Barbara, K.; Paternoster, S.; Arndt, A.; Niemeyer, Christof, M.; Bräuchle, C.; Lamb, Don, C. *Small* **2006**, *2*, 1083−1089.
(13) Hazarika, P.; Ceyhan, B.; Niemeyer, C. M. *Angew. Chem., Int. Ed.* **2004**, *43*, 6469−6471.
(14) Niemeyer, C. M.; Koehler, J.; Wuerdemann, C. *ChemBioChem.* **2002**, *3*, 242−245.

(15) Chhabra, R.; Sharma, J.; Liu, Y.; Yan, H. *Nano Lett.* **2006**, *6*, 978−983.
(16) Kirby, R.; Cho, E. J.; Gehrke, B.; Bayer, T.; Park, Y. S.; Neikirk, D. P.; McDevitt, J. T.; Ellington, A. D. *Anal. Chem.* **2004**, *76*, 4066−4075.
(17) Nutiu, R.; Li, Y. F. *J. Am. Chem. Soc.* **2003**, *125*, 4771−4778.
(18) Stojanovic, M. N.; Kolpashchikov, D. M. *J. Am. Chem. Soc.* **2004**, *126*, 9266−9270.
(19) Benenson, Y.; Gil, B.; Ben-Dor, U.; Adar, R.; Shapiro, E. *Nature* **2004**, *429*, 423−429.
(20) Nutiu, R.; Li, Y. F. *Angew. Chem., Int. Ed.* **2005**, *44*, 5464−5467.
(21) Kolpashchikov, D. M.; Stojanovic, M. N. *J. Am. Chem. Soc.* **2005**, *127*, 11348−11351.
(22) Beyer, S.; Simmel, F. C. *Nucleic Acids Res.* **2006**, *34*, 1581−1587.
(23) Buranachai, C.; McKinney, S. A.; Ha, T. *Nano Lett.* **2006**, *6*, 496−500.
(24) Müller, B. K.; Zaychikov, E.; Brauchle, C.; Lamb, D. C. *Biophys. J.* **2005**, *89*, 3508−3522.
(25) Kapanidis, A. N.; Lee, N. K.; Laurence, T. A.; Doose, S.; Margeat, E.; Weiss, S. *PNAS* **2004**, *101*, 8936−8941.
(26) Förster, T. *Ann. Phys. (Leipzig)* **1948**, *2*, 55−75.
(27) Lakowicz, J. R. *Principles of Fluorescence Spectroscopy*, 2nd ed; Plenum: New York, 1999; p 698.
(28) Zander, C.; Sauer, M.; Do, D.-S.; Ashulz, A.; Wolfrum, J.; Brand, L.; Eggeling, C.; Seidel, C. A. M. *Appl. Phys. B* **1996**, *63*, 517−523.
(29) Fries, J. R.; Brand, L.; Eggeling, C.; Kollner, M.; Seidel, C. A. M. *J. Phys. Chem. A* **1998**, *102*, 6601−6613.
(30) Eggeling, C.; Fries, J. R.; Brand, L.; Gunther, R.; Seidel, C. A. M. *PNAS* **1998**, *95*, 1556−1561.
(31) Lee, N. K.; Kapanidis, A. N.; Wang, Y.; Michalet, X.; Mukhopadhyay, J.; Ebright, R. H.; Weiss, S. *Biophys. J.* **2005**, *88*, 2939−2953.

NL0619406